Dalton Transactions

RSC Publishing

PAPER

View Article Online
View Journal

Cite this: DOI: 10.1039/c3dt51501j

Discrimination of *cis–trans* isomers by dinuclear metal cryptates at physiological pH: selectivity for fumarate *vs.* maleate†

Gao-Yi Xie, Long Jiang and Tong-Bu Lu*

Received 6th June 2013,
Accepted 17th July 2013

DOI: 10.1039/c3dt51501j

www.rsc.org/dalton

Cryptand **L** (**L** = N[$(CH_2)_2NHCH_2$(2,6-$C_{10}H_6$)$CH_2NH(CH_2)_2]_3$N) and its dinuclear metal cryptates $[Zn_2L](NO_3)_4$ (**1**) and $[Cu_2L](ClO_4)_4$ (**2**) have been prepared, and the binding properties of the cryptates with fumarate and its *cis* isomer maleate were investigated using fluorescent spectra, ^{1}H NMR titrations and single crystal X-ray diffraction analysis for $[(Cu_2L)(fum)][ClO_4]_2$ (**3**) (fum = fumarate). Thanks to the size and shape matching effect, the cryptates can selectively recognize fumarate at physiological pH, with an association constant almost 18-fold larger than that of maleate, forming a cradle-like cascade complex.

Introduction

Carefully designed molecular cages (or capsules) with tailored size and shape can provide discrete microenvironments for targeted substrates, and the behavior of the encapsulated substrates diverges substantially from the behavior of free molecules in dilute solution,[1] such as low activation energy,[2] different reactive sites,[3] and reactivity inhibition of unstable molecules or intermediates.[4] Polyaza cryptands and cryptates, as classical cage-like host molecules, draw particular attention, not only due to their facility to be synthesized, but also because of their excellent capabilities in anion recognition and molecule activation.[5] For instance, Fabbrizzi and coworkers[6] found that a dicopper cryptate can selectively recognize 1,4- over 1,2- or 1,3-benzenedicarboxylate. However, to the best of our knowledge, selective recognition of *cis–trans* isomers by a dinuclear cryptate has not been reported so far.

Herein we focus our attention on the recognition of *cis–trans* isomers of fumarate (fum^{2-}) and maleate ($male^{2-}$). The importance of discrimination of fum^{2-} and $male^{2-}$ is not only related to the specific recognition of *cis–trans* isomers, but also due to their conflicting biochemical behavior and the wide application of fumarate in food and pharmaceutical industries.[7] To date, a few synthesized receptors for fum^{2-} and $male^{2-}$ recognition and sensing in solution have been reported;[8] however, all of them worked in either organic solvents or acid aqueous solution; it remains a challenge to selectively recognize fum^{2-} and $male^{2-}$ in aqueous solution at physiological pH. Nevertheless, dinuclear cryptates with specific counter anions may be the perfect receptors for achieving this.

As we know, the recognition of dinuclear cryptates to anions depends on the size matching between the M···M separations in the cryptates and the lengths of anions.[5d] In addition, increasing the rigidity of a cryptate can improve its selectivity to anions, as the M···M distance can be fixed within a narrow range for a rigid cryptate.[9] We previously demonstrated that dinuclear metal cryptates $[M_2L^1]^{4+}$ (M = Cu and Zn) can cleave the C–C bond of nitriles to generate cyanido-bridged complexes $[M_2L^1(CN)]^{3+}$ due to the high recognition of $[M_2L^1]^{4+}$ towards CN^- (the perfect size matching between M···M separations of $[M_2L^1]^{4+}$ and the length of CN^-),[2a,c] and the rigid cryptate $[Co_2L^1]^{4+}$ can recognize Cl^- and Br^- but not F^- and I^-.[9] In order to include longer isomers of fum^{2-} and $male^{2-}$ anions, a cryptand with a longer pole···pole distance is needed. Therefore, we used 2,6-naphthyl instead of phenyl as a spacer to design a new cryptand **L** (Scheme 1). In comparison with $[M_2L^1]^{4+}$ (M = Cu and Zn), $[M_2L]^{4+}$ possesses the following two advantages. (1) $[M_2L]^{4+}$ has longer M···M separations that can include longer anions such as fum^{2-} and $male^{2-}$; (2) 2,6-naphthyl is a fluorescent active group; thus the recognizing process of $[Zn_2L]^{4+}$ towards anions can be monitored by the fluorescent changes of $[Zn_2L]^{4+}$.

Herein, we reported the synthesis and structures of a new cryptand **L** and its two dinuclear cryptates $[M_2L]^{4+}$ (M = Zn and Cu). We found that $[M_2L]^{4+}$ can recognize fum^{2-} over $male^{2-}$ at physiological pH, and the association constant for $[Zn_2L]^{4+}$

MOE Key Laboratory of Bioinorganic and Synthetic Chemistry/State Key Laboratory of Optoelectronic Materials and Technologies/School of Chemistry and Chemical Engineering, Sun Yat-Sen University, Guangzhou 510275, China.
E-mail: lutongbu@mail.sysu.edu.cn; Fax: +86-20-84112921

†Electronic supplementary information (ESI) available: Selected bond distances and angles, NMR and ESI-MS spectra, Job's plot, the structure of **4**. For crystallographic data in CIF (PDF). CCDC 928731–928733 for **3**, **4** and **L**, respectively. For ESI and crystallographic data in CIF or other electronic format see DOI: 10.1039/c3dt51501j

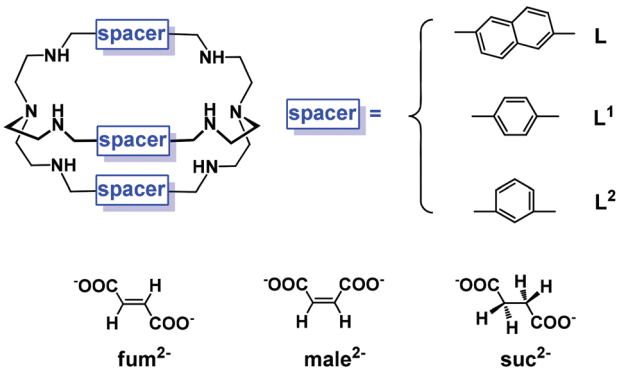

Scheme 1 The structures of cryptands and dicarboxylates.

with fum^{2-} is almost 18 folds larger than that with $male^{2-}$. In aqueous solution, the fluorescence of cryptate $[Zn_2L]^{4+}$ was quenched significantly upon the addition of 50 equiv. of fum^{2-}, but slightly decreased when $male^{2-}$ was added, and NMR titrations and the crystal structure analysis provided further insight into the binding properties between the host and the guest. For comparison, the recognition of $[M_2L]^{4+}$ to suc^{2-}, which has the same number of carbon atoms and a similar structure to fum^{2-}, has also been investigated.

Results and discussion

Synthesis and structure of L

The synthetic route of **L** is illustrated in Scheme 2, in which dimethyl naphthalene-2,6-dicarboxylate (**I**) was reacted with excess $LiAlH_4$ to give 2,6-bis-hydroxymethyl naphthalene (**II**), which was further reacted with excess pyridinium chlorochromate (PCC) to produce naphthalene-2,6-dicarbaldehyde (**III**).

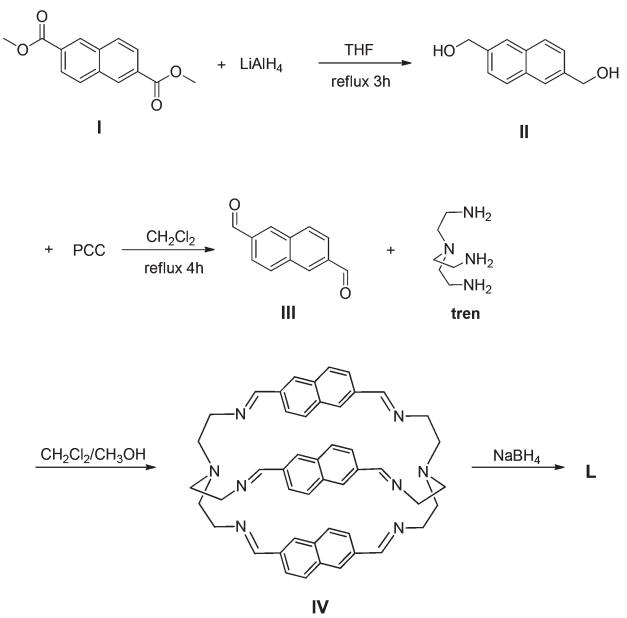

Scheme 2 The synthesis route of **L**.

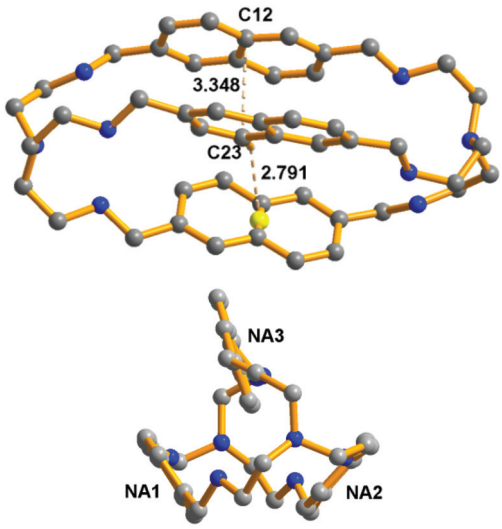

Fig. 1 The single crystal structure of **L**.

After Schiff base condensation of **III** with tris(2-aminoethyl)-amine (tren), followed by hydrogenation with $NaBH_4$ and recrystallization in toluene, the cryptand **L** was obtained in good yield (66%). The structure of **L** was confirmed by nuclear magnetic resonance (NMR) spectroscopy and mass spectrometry (MS) (Fig. S5–S7, ESI†), as well as by X-ray crystallography. As shown in Fig. 1, **L** displays an ellipsoidal structure, with the bridgehead nitrogen distance of 13.343(1) Å. Different from the reported structures of cryptands,[10] there is no 3-fold axis along the two bridgehead nitrogen atoms in **L**, as one of the naphthalene (NA) spacers in **L** (NA3) rotates, with the C(23)–H(23) bond pointing to the cavity of **L**. In addition, NA3 is almost parallel to the second NA spacer (NA1), with the dihedral angle of 14.576° and the shortest C···C distance of 3.348(2) Å (C(12)···C(23)), implying the presence of intramolecular π–π interactions.[11] After the reaction of **L** with $Zn(NO_3)_2{\cdot}6H_2O$/$Cu(ClO_4)_2{\cdot}6H_2O$ in ethanol, $[Zn_2L](NO_3)_4$ (**1**) and $[Cu_2L](ClO_4)_4$ (**2**), which were used as receptors for the *cis–trans* isomers, were obtained.

Fluorescent spectra

The fluorescent spectra of $[Zn_2L]^{4+}$ with fum^{2-} and $male^{2-}$ anions in aqueous solution at physiological pH (HEPES buffer, pH 7.40, 20 mM) were investigated. As shown in Fig. 2, $[Zn_2L]^{4+}$ displays a broad peak at 398 nm, which can be attributed to the excimer emission of NA spacers in $[Zn_2L]^{4+}$. Upon the addition of 50 equiv. of $male^{2-}$, the fluorescence of $[Zn_2L]^{4+}$ slightly decreased; however, significant fluorescent quenching of $[Zn_2L]^{4+}$ was observed when 50 equiv. of fum^{2-} was added, indicating that $[Zn_2L]^{4+}$ can recognize fum^{2-} over $male^{2-}$. Job's plot of $[Zn_2L]^{4+}$ with fum^{2-} at 398 nm displays a maximum fluorescent intensity change value at $[Zn_2L]/\{[Zn_2L] + [fum^{2-}]\} = 0.5$ ($[Zn_2L]$ is the concentration of $[Zn_2L]^{4+}$), indicating that a 1 : 1 inclusion compound was formed (Fig. 3).[12] To quantify the binding constants of $[Zn_2L]^{4+}$ towards fum^{2-} and $male^{2-}$, an aqueous solution of $[Zn_2L]^{4+}$ was titrated with fum^{2-}

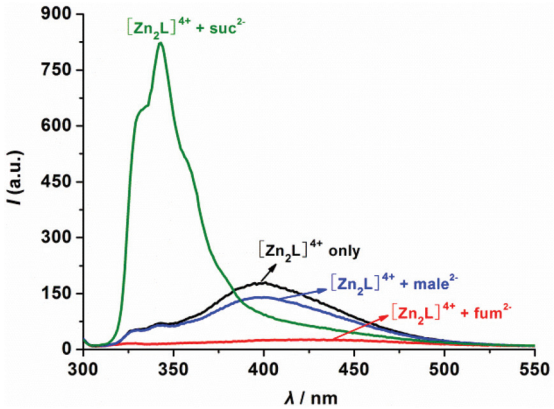

Fig. 2 Fluorescent spectra of $[Zn_2L]^{4+}$ (2×10^{-5} M) upon the addition of 50 equiv. of different dicarboxylates at pH 7.40 (HEPES buffer, 20 mM) (excitation at 290 nm).

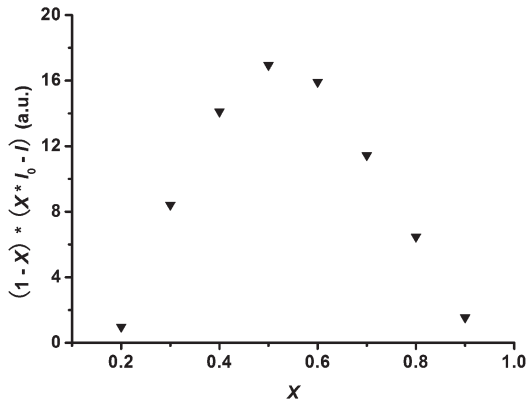

Fig. 3 Job's plot of the complexation between $[Zn_2L]^{4+}$ and fum^{2-} in aqueous solution (HEPES buffer, pH 7.40, 20 mM). Total concentration of $[Zn_2L]^{4+}$ and fum^{2-} was kept constant at 4×10^{-5} M. $X = [Zn_2L]/\{[Zn_2L] + [fum^{2-}]\}$.

(or $male^{2-}$), giving two K_a values of $(4.3 \pm 0.5) \times 10^4$ M^{-1} (R^2 = 0.9911) and $(2.3 \pm 0.3) \times 10^3$ M^{-1} (R^2 = 0.9974) for fum^{2-} and $male^{2-}$, respectively (Fig. 4a and 4b).[13] Obviously, the binding selectivity is not a consequence of the different acidities/basicities of fum^2 *vs.* $male^{2-}$, as both fumaric and maleic acids are deprotonated at pH 7.40.[8c]

We postulate that both fum^{2-} and $male^{2-}$ can coordinate with two Zn^{2+} cations in $[Zn_2L]^{4+}$, and the fluorescence quenching effect by the two guests is caused by π–π stacking interactions between NA spacers of $[Zn_2L]^{4+}$ and the C=C bond of the guests, through an energy transfer process.[14] The selectivity for fum^{2-} over its *cis* isomer $male^{2-}$ is due to the geometrical factor; the extended conformation of fum^{2-} makes it more suitable to coordinate with two Zn^{2+} cations in $[Zn_2L]^{4+}$. To demonstrate this assumption, fluorescent spectra of $[Zn_2L]^{4+}$ with suc^{2-} were also investigated. As shown in Fig. 2, the addition of 50 equiv. of suc^{2-} induced the disappearance of the excimer emission and a large enhancement of the monomer emission (343 nm) of NA spacers in $[Zn_2L]^{4+}$. This can be explained by the isolation effect of bound suc^{2-},[15]

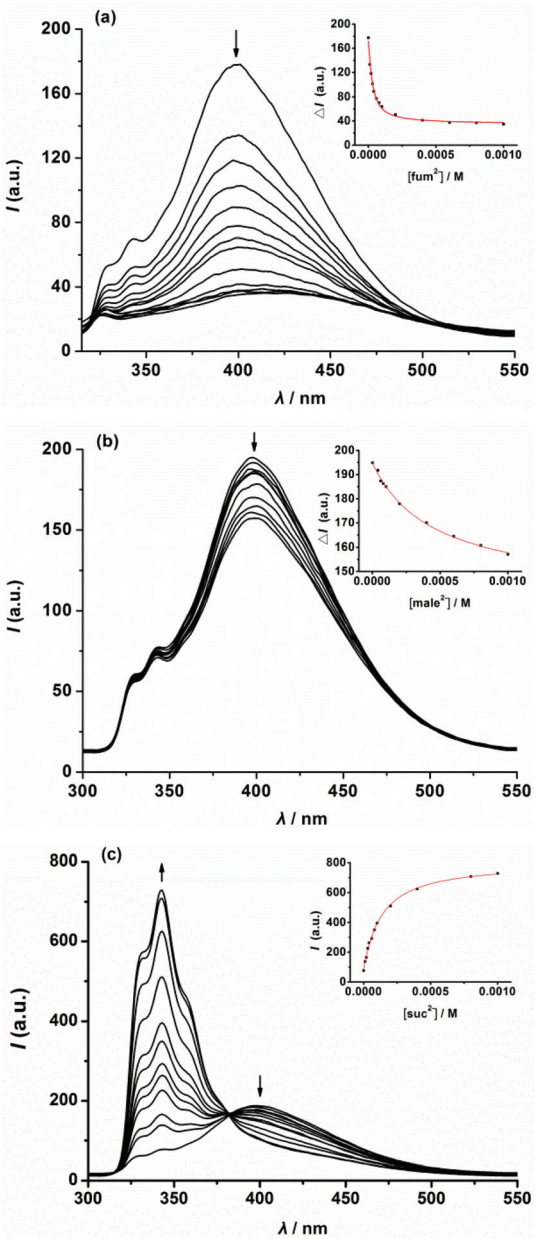

Fig. 4 Fluorescent titration of $[Zn_2L]^{4+}$ (2×10^{-5} M) upon the addition of (a) fum^{2-}, (b) $male^{2-}$, (c) suc^{2-} in aqueous solution (HEPES buffer, pH 7.40, 20 mM) (excitation at 290 nm). Inset: curve-fitting analysis of the fluorescence emission change at 398 nm (for fum^{2-} and $male^{2-}$) or 343 nm (for suc^{2-}).

which prohibits the π–π interactions between two NA spacers of $[Zn_2L]^{4+}$. Thus the fluorescent quenching of $[Zn_2L]^{4+}$ by fum^{2-} can be attributed to the π–π stacking interactions between NA spacers in $[Zn_2L]^{4+}$ and the C=C bond in fum^{2-}. Job's plot of $[Zn_2L]^{4+}$ with suc^{2-} at 343 nm (Fig. S8, ESI†) also displays a 1 : 1 binding stoichiometry, and the fluorescent titration of $[Zn_2L]^{4+}$ with suc^{2-} (Fig. 4c) gave a K_a value of $(8.0 \pm 0.5) \times 10^3$ M^{-1} (R^2 = 0.9983). The smaller K_a value for suc^{2-} relative to fum^{2-} may be due to the more flexible structure of suc^{2-} and the lack of π–π stacking interactions between NA spacers in $[Zn_2L]^{4+}$ and suc^{2-}.

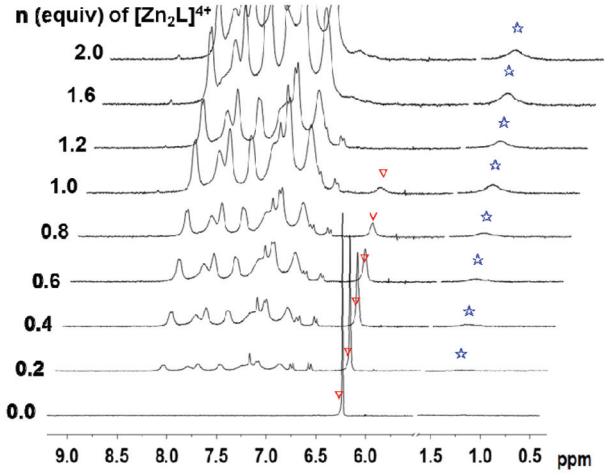

Fig. 5 ^{1}H NMR titration of fum^{2-} (0.011 M) with increasing concentrations of $[Zn_2L]^{4+}$ in DMSO-d_6–D_2O (2 : 1 v/v, pH 7.4). (▽) methine signals in free fum^{2-}; (☆) methine signals in bound fum^{2-}.

^{1}H NMR spectra

To get further insight into the binding properties of $[Zn_2L]^{4+}$, ^{1}H NMR titrations of the three dicarboxylates with $[Zn_2L]^{4+}$ in DMSO-d_6–D_2O (2 : 1 v/v) were carried out. As shown in Fig. 5, upon the addition of $[Zn_2L]^{4+}$, the signals of –HC═C*H*– (6.23 ppm) in free fum^{2-} decreased in intensity, and almost disappeared when 1 equiv. of $[Zn_2L]^{4+}$ was added, which is in good agreement with the result of Job's plot in fluorescence experiment. Meanwhile, a broad peak at 1.28 ppm was observed, which can be assigned to the bound fum^{2-}. Similar changes were observed when $[Zn_2L]^{4+}$ was added into suc^{2-}, and signals of –H_2C–CH_2– (2.10 ppm) in free suc^{2-} disappeared, accompanied by the appearance of a broad peak (–1.42 ppm) assigned to the bound suc^{2-} (Fig. S9, ESI†). In contrast, the addition of $[Zn_2L]^{4+}$ into male^{2-} resulted in downfield shifts ($\Delta\delta \leq 0.37$ ppm) and decreased intensity of the –HC═C*H*– signals, but the methine signals of male^{2-} did not disappear even when 2 equiv. of $[Zn_2L]^{4+}$ was added (Fig. S10, ESI†). The results of ^{1}H NMR experiments indicate that both fum^{2-} and suc^{2-} (rather than male^{2-}) can be encapsulated within the cavity of $[Zn_2L]^{4+}$, as the separate signals for free and bound guests, as well as the large upfield shifts of the signals in the bound guest, are characteristic of the encapsulated guest in a cage with aromatic subunits.[4c,16]

X-ray crystal structures

Though we failed to get single crystals of $[Zn_2L]^{4+}$ with dicarboxylate, the single crystals of $[(Cu_2L)(fum)][ClO_4]_2(CH_3CN)_3(H_2O)$ (**3**·3CH_3CN·H_2O) and $[(Cu_2L)(suc)][ClO_4]_2(CH_3CN)_3(H_2O)_{0.5}$ (**4**·3CH_3CN·0.5H_2O) were successfully obtained by slowly evaporating an acetonitrile–water (4 : 1 v/v) solution containing $[Cu_2L](ClO_4)_4$ and fum^{2-} (or suc^{2-}) in the open air. Both **3** and **4** crystallize in space group $P2_1/n$ (Table 1), forming a similar structure. As shown in Fig. 6, S11 and S12,† two Cu^{2+} cations in **3** (or **4**) are bridged by one fum^{2-} (or suc^{2-}) anion, with a Cu···Cu separation of 8.769(2) Å (or 8.773(1) Å), and the C(50)–C(51) distance of 1.290(10) Å (or 1.505(8) Å). The fum^{2-} (or suc^{2-}) is encapsulated into the cavity of $[Cu_2L]^{4+}$, displaying a cradle-like structure. In both cryptates, each Cu^{2+} cation is five-coordinated with four nitrogen atoms of **L** and one oxygen atom of fum^{2-} (or suc^{2-}). The average Cu–O (coordinated) distance in **3** is almost equal to that in **4** (Table S1, ESI†). In addition, the plane of the fum^{2-} anion is subparallel to the two side NA spacers, with the dihedral angles of 5.145° and 10.781°, respectively, and the centroid···centroid (Fig. 6) distances between them are 3.432 Å

Table 1 Crystal data and structure refinements for **L**, **3**·3CH_3CN·H_2O and **4**·3CH_3CN·0.5H_2O

Compound	**L**	**3**·3CH_3CN·H_2O	**4**·3CH_3CN·0.5H_2O
Formula	$C_{48}H_{60}N_8$	$C_{58}H_{73}Cl_2Cu_2N_{11}O_{13}$	$C_{58}H_{74}Cl_2Cu_2N_{11}O_{12.5}$
fw	749.04	1330.25	1323.26
Crystal system	Orthorhombic	Monoclinic	Monoclinic
T (K)	150(2)	150(2)	150(2)
Space group	$P2_12_12_1$	$P2_1/n$	$P2_1/n$
a/Å	9.4145(1)	18.3034(7)	18.3486(7)
b/Å	14.9511(2)	9.9708(2)	10.0477(2)
c/Å	29.1625(4)	32.6485(10)	32.7258(10)
α/°	90	90	90
β/°	90	99.563(3)	99.934(3)
γ/°	90	90	90
V/Å^3, Z	4104.85(9), 4	5875.5(3), 4	5942.9(3), 4
F (000)	1616	2776	2764
Crystal size/mm^3	0.33 × 0.25 × 0.20	0.37 × 0.30 × 0.21	0.31 × 0.27 × 0.22
Reflns collected/unique (R_{int})	32 134/7258 (R_{int} = 0.0212)	19 505/8608 (R_{int} = 0.0516)	19 009/9711 (R_{int} = 0.0499)
Obsd reflns [$I \geq 2\sigma(I)$]	7132	6084	6737
Data/restraints/parameter	7258/0/529	8608/53/1018	9711/61/1015
D_c/Mg m^{-3}	1.212	1.504	1.479
μ/mm^{-1}	0.559	2.351	2.314
Goodness-of-fit on F^2	1.062	1.099	1.039
R_1,[a] wR_2 [b] [$I \geq 2\sigma(I)$]	0.0276/0.0686	0.0919, 0.2131	0.0749, 0.1713
R_1, wR_2 (all data)	0.0282/0.0692	0.1230, 0.2330	0.1111, 0.1964

[a] $R_1 = \sum||F_o| - |F_c||/\sum|F_o|$. [b] $wR_2 = [\sum[w(F_o^2 - F_c^2)^2]/\sum w(F_o^2)^2]^{1/2}$, where $w = 1/[\sigma^2(F_o)^2 + (aP)^2 + bP]$ and $P = (F_o^2 + 2F_c^2)/3$.

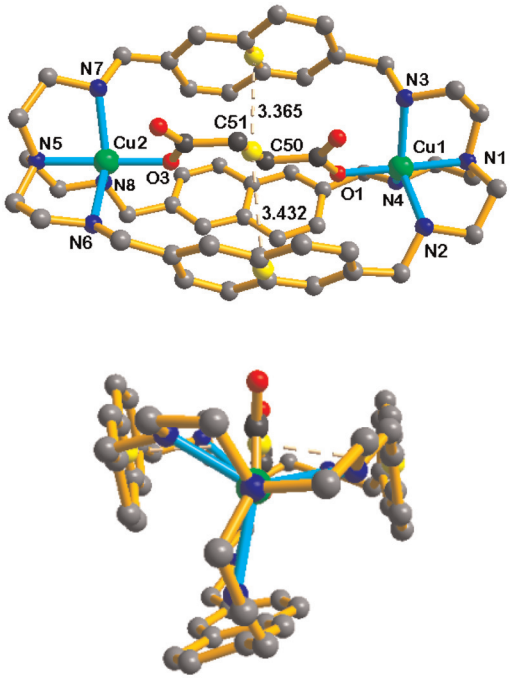

Fig. 6 The structure of the $[(Cu_2L)(fum)]^{2+}$ cation in **3**.

and 3.365 Å, respectively, demonstrating that there are π–π stacking interactions between fum^{2-} and the NA spacers in $[Cu_2L]^{4+}$.[14a,17] No obvious Jahn–Teller distortion is observed in **3** and **4**, as all the Cu(II) ions in **3** and **4** are five-coordinated, with a trigonal bipyramidal rather than octahedral geometry. We believe that the structures of $[(Zn_2L)(fum)]^{2+}$ and $[(Zn_2L)(suc)]^{2+}$ should be similar to those of **3** and **4**, respectively, as most of the reported structures of five-coordinated Zn(II) cryptates of $\mathbf{L}^1$ and $\mathbf{L}^2$ are similar to those of five-coordinated Cu(II) cryptates.[2a,c,18]

Conclusion

In conclusion, we have reported a dicarboxylate encapsulation by rigid $[M_2L]^{4+}$ in aqueous solution at physiological pH, with selectivity for fum^{2-} over its *cis* isomer $male^{2-}$, due to the size and shape matching effect. The results of ^{1}H NMR spectra and the crystal structure analysis demonstrate that fum^{2-} can be encapsulated within the cavity of $[M_2L]^{4+}$. The extended and rigid conformation, as well as the right size of fum^{2-}, makes it perfectly coordinate with two Zn^{2+} (or Cu^{2+}) cations in $[M_2L]^{4+}$; the π–π stacking interactions also enhance the affinity of $[M_2L]^{4+}$ towards fum^{2-}.

Experimental

All chemicals were commercially available and used without further purification. ^{1}H NMR spectra were recorded using a Varian Mercury 300 spectrometer. ESI-MS analysis was performed using a Thermo Finigan LCQDECA XP HPLC-MSn mass spectrometer. Elemental analyses were determined using an Elementar Vario EL elemental analyzer. The IR spectra were recorded in the 4000–400 cm^{-1} region in the form of KBr pellets using a Bruker EQUINOX 55 spectrometer. Fluorescent spectra were recorded using a Shimadzu RF-5301PC spectrofluorophotometer.

Synthesis of L

2,6-Bis-hydroxymethyl naphthalene (II). To an ice-cooled solution of dimethyl naphthalene-2,6-dicarboxylate (3.66 g, 15 mmol) in dry THF (150 mL) under nitrogen, $LiAlH_4$ (2.28 g, 60 mmol) was added carefully. The reaction was allowed to reach room temperature for 40 min, and then was warmed up to 343 K for 3 h. The mixture was carefully treated in sequence with 2.3 mL of water, 2.3 mL of a 15% NaOH aqueous solution, and 6.8 mL of water, and then the suspension was filtered and the solution was evaporated to yield a white solid (2.73 g, 97%). ^{1}H NMR of 2,6-bis-hydroxymethyl naphthalene (300 MHz, DMSO-d_6) δ 4.64 (4H, d, J = 5.67 Hz), 5.28 (2H, t, J = 5.71 Hz), 7.43 (2H, d, J = 8.35 Hz), 7.77 (2H, s), 7.82 (2H, d, J = 8.52 Hz). ^{13}C NMR of 2,6-bis-hydroxymethyl naphthalene (75 MHz, DMSO-d_6, TMS) δ 63.8, 124.9, 126.0, 128.1, 132.7, 140.3.

Naphthalene-2,6-dicarbaldehyde (III). To a stirred suspension of pyridinium chlorochromate (9.67 g, 43.9 mmol) in anhydrous CH_2Cl_2 (100 mL) at 323 K under nitrogen, a suspension of 2,6-bis-hydroxymethyl naphthalene (2.73 g, 14.5 mmol) in anhydrous CH_2Cl_2 (50 mL) was added in one portion. The reaction mixture was rigorously stirred for 4 h at 323 K, and then cooled to room temperature and poured into cold diethyl ether (500 mL). The mixture was triturated until the tar solidified and then filtered through a large pad of silica, eluting with an additional portion of ether (200 mL). The solvents were removed by evaporation, water (200 mL) was added, and the resulting solution was extracted with CH_2Cl_2 (3 × 50 mL), and the organic layer was dried over $MgSO_4$ and evaporated to yield naphthalene-2,6-dicarbaldehyde as a white solid (2.12 g, 79%). ^{1}H NMR of naphthalene-2,6-dicarbaldehyde (300 MHz, $CDCl_3$) δ 8.04 (2H, d, J = 8.46 Hz), 8.11 (2H, d, J = 8.48 Hz), 7.39 (2H, s), 10.20 (2H, s). ^{13}C NMR of naphthalene-2,6-dicarbaldehyde (75 MHz, $CDCl_3$, TMS) δ 124.3, 130.8, 133.8, 135.9, 136.4, 191.8.

Cryptand L. To a solution of naphthalene-2,6-dicarbaldehyde (0.828 g, 4.5 mmol) in CH_2Cl_2 (300 mL) at room temperature, a solution of tris(2-aminoethyl)amine (0.452 g, 3 mmol) in CH_3OH (300 mL) was added dropwise within 10 h. After the addition was completed, the mixture was stirred for 24 h, the solution was concentrated to about 200 mL by evaporation, and $NaBH_4$ (1.22 g, 32.2 mmol) was added carefully under stirring. After stirring at 323 K for 12 h, the solvent was removed by evaporation, and water (100 mL) was added, the resulting solution was extracted with CH_2Cl_2 (3 × 50 mL), the organic layer was dried over Na_2SO_4 and dried by evaporation, and then recrystallized in toluene (10 mL) to form pale yellow crystals (0.749 g, 66%). ^{1}H NMR of **L** (300 MHz, $CDCl_3$) δ 2.69–2.80 (12H, m), 2.93–3.05 (12H, m), 3.89 (12H, s), 6.60 (6H, d,

J = 8.33), 6.85 (6H, d, J = 8.31), 7.33 (6H, s). ^{13}C NMR of **L** (75 MHz, $CDCl_3$, TMS) δ 47.7, 52.7, 55.0, 125.2, 125.9, 128.0, 132.6, 137.1. MS (ESI) of **L**: m/z 375.6 ($[H_2L]^{2+}$); 749.6 ($[HL]^{+}$). Elemental analysis (%) calcd for $C_{48}H_{60}N_8$ (**L**): C 76.97, H 8.07, N 14.96; found: C 77.00, H 8.03, N 14.86; IR (KBr, cm^{-1}): 3438 m, 3282 s, 3049 m, 2939 s, 2872 s, 2800 s, 2661 m, 2633 m, 1923w, 1773w, 1606 m, 1503 m, 1453 s, 1346 m, 1315 s, 1283 m, 1214 m, 1158 m, 1129 s, 1054 s, 992 m, 918 m, 817 s, 790 m, 745 s, 651 m, 480 s.

Synthesis of the complexes

$[Zn_2L](NO_3)_4$ (1). A solution of $Zn(NO_3)_2{\cdot}6H_2O$ (264 mg, 0.8 mmol) in anhydrous ethanol (10 mL) was added to a solution of **L** (200 mg, 0.267 mmol) in anhydrous ethanol (30 mL). The resulting mixture was stirred at room temperature for 20 min, and a large amount of white precipitate was formed. The precipitate was filtered, washed with anhydrous ethanol, and dried under vacuum. Yield: 260 mg, 81% based on **L**. Elemental analysis (%) calcd for $C_{48}H_{68}N_{12}Zn_2O_{16}$ (**1**·$4H_2O$): C 48.04, H 5.71, N 14.01; found: C 48.16, H 5.73, N 13.88.

$[Cu_2L](ClO_4)_4$ (2). This complex was prepared by a similar procedure to that of **1** from $Cu(ClO_4)_2{\cdot}6H_2O$ and **L** in 85% yield. Elemental analysis (%) calcd for $C_{48}H_{80}Cl_4Cu_2N_8O_{26}$ (**2**·$10H_2O$): C 39.65, H 5.55, N 7.71; found: C 39.17, H 5.12, N 7.83.

$[Cu_2L(fum)][ClO_4]_2$ (3). A solution of **2**·$10H_2O$ (45 mg, 0.031 mmol) in acetonitrile (12 mL) was added dropwise to a solution of disodium fumarate (9.0 mg, 0.056 mmol) in acetonitrile–water (3 : 1, 4 mL). The mixture was stirred at room temperature for 20 min. The resulting solution was filtered and evaporated slowly at room temperature to give blue crystals of **3**·$3CH_3CN{\cdot}H_2O$ (10 mg, 24%). The acetonitrile molecules in the crystals were partly lost upon exposure to the atmosphere. Elemental analysis (%) calcd for $C_{54}H_{75}Cl_2Cu_2N_9O_{17}$ (**3**·$CH_3CN{\cdot}5H_2O$): C 49.13, H 5.73, N 9.55; found: C 49.03, H 5.52, N 9.02; IR (KBr, cm^{-1}): 3407 s, 3257 s, 3048w, 2918 m, 2874 m, 2025w, 1600 m, 1558 s (C═O), 1511w, 1469 m, 1443 s, 1366 s (C═C), 1301 m, 1275w, 1207w, 1083 s (ClO_4^-), 1012 m, 978 m, 947 m, 916 m, 891 m, 860 m, 817 m, 798 m, 695 m, 624 s, 479 m.

$[Cu_2L(suc)][ClO_4]_2$ (4). The crystals of $[Cu_2L(suc)][ClO_4]_2(CH_3CN)_3(H_2O)_{0.5}$ were obtained by a similar procedure to that of **3**·$3CH_3CN{\cdot}H_2O$ from **2**·$10H_2O$ and disodium succinate hexahydrate in 30% yield. The acetonitrile molecules in the crystals were partly lost upon exposure to the atmosphere. Elemental analysis (%) calcd for $C_{56}H_{76}Cl_2Cu_2N_{10}O_{15}$ (**4**·$2CH_3CN{\cdot}3H_2O$): C 50.68, H 5.77, N 10.55; found: C 50.88, H 5.74, N 10.44; IR (KBr, cm^{-1}): 3408 s, 3259 s, 3050w, 2920 m, 2874 m, 2023w, 1613 m, 1547 s (C═O), 1510w, 1469 m, 1442 m, 1418 m, 1404 m, 1382 m, 1353 m, 1301 m, 1275w, 1221 m, 1084 s (ClO_4^-), 1011 m, 970 m, 947 m, 916 m, 890 m, 860 m, 817 m, 750w, 684 m, 624 s, 481 m.

X-ray crystallography

Single-crystal X-ray diffraction data for the ligand L and the complexes **3**·$3CH_3CN{\cdot}H_2O$ and **4**·$3CH_3CN{\cdot}0.5H_2O$ were collected at 150(2) K on an Agilent Technologies Gemini A Ultra system, with Cu-Kα radiation (λ = 1.54178 Å). The empirical absorption corrections were applied using spherical harmonics, implemented in the SCALE3 ABSPACK scaling algorithm.[19] The structures were solved by direct methods, which yielded the positions of all nonhydrogen atoms. These were refined first isotropically and then anisotropically. All the hydrogen atoms (except those of water molecules) were placed in calculated positions with fixed isotropic thermal parameters and included in structure factor calculations in the final stage of full-matrix least-squares refinement. One of the naphthalene spacers, two ClO_4^- anions and two acetonitrile molecules in both **3**·$3CH_3CN{\cdot}H_2O$ and **4**·$3CH_3CN{\cdot}0.5H_2O$ are disordered, and various restraints (DFIX and SADI) were used to impose equal bond lengths for disordered corresponding parts. The thermal displacement parameters were refined anisotropically and set equal with various constraints (ISOR, DELU and EADP). Hydrogen atoms of disordered acetonitrile molecules were not added. A half water molecule in both **3**·$3CH_3CN{\cdot}H_2O$ and **4**·$3CH_3CN{\cdot}0.5H_2O$, which was refined isotropically, is disordered, and hydrogen atoms of water molecules were not added. All calculations were performed using the SHELXTL system of computer programs.[20] The crystallographic data for **L**, **3**·$3CH_3CN{\cdot}H_2O$ and **4**·$3CH_3CN{\cdot}0.5H_2O$ are summarized in Table 1, and selected bond distances and angles for **3**·$3CH_3CN{\cdot}H_2O$ and **4**·$3CH_3CN{\cdot}0.5H_2O$ are provided in Table S1.†

Fluorescent experiments

Stock solutions of $[Zn_2L]^{4+}$ (0.0008 M) and the sodium salt of different dicarboxylates (0.02 M) were prepared in aqueous solution (HEPES buffer, pH 7.40, 20 mM). A 250 μL solution of $[Zn_2L]^{4+}$ and a 500 μL solution of the substrate (or without substrate) were added into a 10 mL volumetric flask, and then extra HEPES buffer was added to adjust the concentration of $[Zn_2L]^{4+}$ to 2×10^{-5} M, and then the fluorescent experiments were performed.

Fluorescent titration experiments of $[Zn_2L]^{4+}$ with different dicarboxylates were performed in aqueous solution (HEPES buffer, pH 7.40, 20 mM) at room temperature. The association constant (K_a) of $[Zn_2L]^{4+}$ with fum^{2-} or $male^{2-}$ was calculated from the changes of the fluorescent intensities of $[Zn_2L]^{4+}$ at λ_{em} 398 nm using a nonlinear curve-fitting and eqn (1):

$$I = I_0 - \frac{I_0 - I_{min}}{2[H_0]}\left\{\left([H_0] + [G_0] + \frac{1}{K_a}\right) - \sqrt{\left([H_0] + [G_0] + \frac{1}{K_a}\right)^2 - 4[H_0][G_0]}\right\} \quad (1)$$

where I is the intensity of $[Zn_2L]^{4+}$ at 398 nm in the presence of the guest, I_0 is the initial intensity of $[Zn_2L]^{4+}$ at 398 nm without the guest, I_{min} is the intensity of $[Zn_2L]^{4+}$ at 398 nm in the presence of excess amount of the guest, $[H_0]$ is the concentration of $[Zn_2L]^{4+}$, $[G_0]$ is the concentration of the guest, K_a = [complex]/{$[H_0] \times [G_0]$}.

The association constant (K_a) of $[Zn_2L]^{4+}$ with suc^{2-} was calculated from the changes of the fluorescent intensities of $[Zn_2L]^{4+}$ at λ_{em} 343 nm using a nonlinear curve-fitting and eqn (2):

$$I = I_0 + \frac{I_{max} - I_0}{2[H_0]}\left\{\left([H_0] + [G_0] + \frac{1}{K_a}\right) - \sqrt{\left([H_0] + [G_0] + \frac{1}{K_a}\right)^2 - 4[H_0][G_0]}\right\} \quad (2)$$

where I is the intensity of $[Zn_2L]^{4+}$ at 343 nm in the presence of the guest, I_0 is the initial intensity of $[Zn_2L]^{4+}$ at 343 nm without the guest, I_{max} is the intensity of $[Zn_2L]^{4+}$ at 343 nm in the presence of excess amount of the guest, $[H_0]$ is the concentration of $[Zn_2L]^{4+}$, $[G_0]$ is the concentration of the guest, K_a = [complex]/{$[H_0] \times [G_0]$}.

Nonlinear curve-fitting tools of the Origin© (v.7.5) package were used for calculating the value of K_a.

Job's plots

Stock solutions of $[Zn_2L]^{4+}$ (0.0008 M) and the sodium salt of different dicarboxylates (0.0008 M) were prepared in aqueous solution (HEPES buffer, pH 7.40, 20 mM). Ten volumetric flasks (10 mL) were filled with 500 μL solutions of the receptor and the substrate in the following volume ratios: 50 : 450, 100 : 400, 150 : 350, 200 : 300, 250 : 250, 300 : 200, 350 : 150, 400 : 100, 450 : 50 and 500 : 0, and then extra HEPES buffer was added to adjust the total concentration of the receptor and the substrate to 4×10^{-5} M, and the corresponding fluorescence emission curves were recorded.

For fum^{2-}: a plot according to $(1 - X) \times (X \times I_0 - I)$ *versus* X was made, where X is the mole fraction of $[Zn_2L]^{4+}$, I_0 is the initial fluorescence intensity at 398 nm without the addition of the substrate, and I is the fluorescence intensity of $[Zn_2L]^{4+}$ at 398 nm upon the addition of the substrate.

For suc^{2-}: a plot according to $(1 - X) \times (I - X \times I_0)$ *versus* X was made, where X is the mole fraction of $[Zn_2L]^{4+}$, I_0 is the initial fluorescence intensity at 343 nm without the addition of the substrate, and I is the fluorescence intensity of $[Zn_2L]^{4+}$ at 343 nm upon the addition of the substrate.

^{1}H NMR titration experiments

^{1}H NMR titration experiments of dicarboxylates with $[Zn_2L]^{4+}$ were performed in DMSO-d_6–D_2O (2 : 1 v/v, pH 7.40) at room temperature. The NMR solution of dicarboxylates ($C \sim 0.011$ M) was titrated in the NMR tubes with a stock solution of $[Zn_2L]^{4+}$ ($C \sim 0.03$ M). 9–10 data points were recorded.

Acknowledgements

This work was supported by 973 Program of China (2012CB821705) and NSFC (grant no. 91127002, 21121061, and 20831005), and NSF of Guangdong Province (S2012030006240).

References

1 (*a*) T. S. Koblenz, J. Wassenaar and J. N. H. Reek, *Chem. Soc. Rev.*, 2008, **37**, 247; (*b*) Y. Liu, X. Wu, C. He, R. Zhang and C. Duan, *Dalton Trans.*, 2008, 5866; (*c*) M. Yoshizawa, J. K. Klosterman and M. Fujita, *Angew. Chem., Int. Ed.*, 2009, **48**, 3418; (*d*) B. Breiner, J. K. Clegg and J. R. Nitschke, *Chem. Sci.*, 2011, **2**, 51; (*e*) L. Adriaenssens and P. Ballester, *Chem. Soc. Rev.*, 2013, **42**, 3261.

2 (*a*) T. Lu, X. Zhuang, Y. Li and S. Chen, *J. Am. Chem. Soc.*, 2004, **126**, 4760; (*b*) F. R. Pinacho Crisóstomo, A. Lledó, S. R. Shenoy, T. Iwasawa and J. Rebek Jr., *J. Am. Chem. Soc.*, 2009, **131**, 7402; (*c*) L.-Z. Yang, Y. Li, X.-M. Zhuang, L. Jiang, J.-M. Chen, R. L. Luck and T.-B. Lu, *Chem.–Eur. J.*, 2009, **15**, 12399; (*d*) W. M. Hart-Cooper, K. N. Clary, F. D. Toste, R. G. Bergman and K. N. Raymond, *J. Am. Chem. Soc.*, 2012, **134**, 17873; (*e*) C. He, J. Wang, L. Zhao, T. Liu, J. Zhang and C. Duan, *Chem. Commun.*, 2013, **49**, 627.

3 (*a*) A. Natarajan, L. S. Kaanumalle, S. Jockusch, C. L. D. Gibb, B. C. Gibb, N. J. Turro and V. Ramamurthy, *J. Am. Chem. Soc.*, 2007, **129**, 4132; (*b*) R. M. Yebeutchou and E. Dalcanale, *J. Am. Chem. Soc.*, 2009, **131**, 2452; (*c*) T. Murase, S. Horiuchi and M. Fujita, *J. Am. Chem. Soc.*, 2010, **132**, 2866.

4 (*a*) T. Iwasawa, R. J. Hooley and J. Rebek Jr., *Science*, 2007, **317**, 493; (*b*) P. Mal, B. Breiner, K. Rissanen and J. R. Nitschke, *Science*, 2009, **324**, 1697; (*c*) K. Kurotobi and Y. Murata, *Science*, 2011, **333**, 613; (*d*) M. M. J. Smulders and J. R. Nitschke, *Chem. Sci.*, 2012, **3**, 785; (*e*) C.-Y. Gao, L. Zhao and M.-X. Wang, *J. Am. Chem. Soc.*, 2011, **134**, 824.

5 (*a*) V. McKee, J. Nelson and R. M. Town, *Chem. Soc. Rev.*, 2003, **32**, 309; (*b*) E. J. O'Neil and B. D. Smith, *Coord. Chem. Rev.*, 2006, **250**, 3068; (*c*) S. O. Kang, J. M. Llinares, V. W. Day and K. Bowman-James, *Chem. Soc. Rev.*, 2010, **39**, 3980; (*d*) L. Fabbrizzi and A. Poggi, *Chem. Soc. Rev.*, 2012, **42**, 1681.

6 M. Boiocchi, M. Bonizzoni, L. Fabbrizzi, G. Piovani and A. Taglietti, *Angew. Chem., Int. Ed.*, 2004, **43**, 3847.

7 (*a*) G. Latini, *Clin. Chim. Acta*, 2005, **361**, 20; (*b*) U. Heudorf, V. Mersch-Sundermann and J. Angerer, *Int. J. Hyg. Environ. Health*, 2007, **210**, 623; (*c*) S. Eiam-ong, M. Spohn, N. A. Kurtzman and S. Sabatini, *Kidney Int.*, 1995, **48**, 1542; (*d*) K. Uzarevic, I. Halasz, I. Dilovic, N. Bregovic, M. Rubcic, D. Matkovic-Calogovic and V. Tomisic, *Angew. Chem., Int. Ed.*, 2013, **52**, 5504.

8 (*a*) A. M. Costero, M. Colera, P. Gavina and S. Gil, *Chem. Commun.*, 2006, 761; (*b*) Y.-P. Tseng, G.-M. Tu, C.-H. Lin, C.-T. Chang, C.-Y. Lin and Y.-P. Yen, *Org. Biomol. Chem.*, 2007, **5**, 3592; (*c*) P. Mateus, R. Delgado, P. Brandão and V. Félix, *J. Org. Chem.*, 2012, **77**, 4611.

9 J.-M. Chen, X.-M. Zhuang, L.-Z. Yang, L. Jiang, X.-L. Feng and T.-B. Lu, *Inorg. Chem.*, 2008, **47**, 3158.

10 (*a*) F. Arnaud-Neu, S. Fuangswasdi, B. Maubert, J. Nelson and V. McKee, *Inorg. Chem.*, 2000, **39**, 573; (*b*) P. S. Lakshminarayanan, E. Suresh and P. Ghosh,

J. Am. Chem. Soc., 2005, **127**, 13132; (*c*) I. Ravikumar, P. S. Lakshminarayanan, E. Suresh and P. Ghosh, *Inorg. Chem.*, 2008, **47**, 7992.

11 H. M. Colquhoun, Z. Zhu and D. J. Williams, *Org. Lett.*, 2003, **5**, 4353.

12 K.-H. Chen, J.-H. Liao, H.-Y. Chan and J.-M. Fang, *J. Org. Chem.*, 2008, **74**, 895.

13 Y. Shiraishi, S. Sumiya and T. Hirai, *Chem. Commun.*, 2011, **47**, 4953.

14 (*a*) J. Nelson, M. Nieuwenhuyzen, I. Pal and R. M. Town, *Chem. Commun.*, 2002, 2266; (*b*) J. J. Gassensmith, E. Arunkumar, L. Barr, J. M. Baumes, K. M. DiVittorio, J. R. Johnson, B. C. Noll and B. D. Smith, *J. Am. Chem. Soc.*, 2007, **129**, 15054; (*c*) J. W. G. Bloom and S. E. Wheeler, *Angew. Chem., Int. Ed.*, 2011, **50**, 7847.

15 Z. Xu, N. J. Singh, J. Lim, J. Pan, H. N. Kim, S. Park, K. S. Kim and J. Yoon, *J. Am. Chem. Soc.*, 2009, **131**, 15528.

16 (*a*) J. Rebek Jr., *Angew. Chem., Int. Ed.*, 2005, **44**, 2068; (*b*) H. Gan and B. C. Gibb, *Chem. Commun.*, 2013, **49**, 1395.

17 Y. Inoue, T. Kanbara and T. Yamamoto, *Tetrahedron Lett.*, 2004, **45**, 4603.

18 Y. Dussart, C. Harding, P. Dalgaard, C. McKenzie, R. Kadirvelraj, V. McKee and J. Nelson, *J. Chem. Soc., Dalton Trans.*, 2002, 1704.

19 *CrysAlis RED, Version 1.171.31.7*, Oxford Diffraction Ltd, 2006.

20 G. M. Sheldrick, *SHELXTL-97: Program for crystal structure solution and refinement*, University of Göttingen, Germany, 1997.

